Journal of the Korean Nuclear Society
Volume 17, Number 2, June 1985

Axial Height-Dependent Transverse Buckling Model for 1-Dimensional Analysis of Load Follow Operation

Ho Ju Moon and Sung Ki Chae
Korea Advanced Energy Research Institute
(Received April 2, 1985)

일차원적 부하추종 운전해석을 위한 축방향높이 의존적 중성자속 버클링 모델

문 호 주·채 성 기
한국에너지연구소
(1985. 4. 2 접수)

Abstract

The axial height-dependent transverse buckliing is derived from 3-dimensional depletion file in steadystate conditions. For transient conditions a physical correlation is developed based on the linear relationship existing between the responses of in-core and ex-core detectors. The use of this model greatly improves the reliability of a 1-dimensional diffusion theory program in predicting the axial power transients accompanying large variations of control rod positions.

요 약

정상상태하의 축방향높이 의존적 중성자속 버클링은 3차원적연소 이력자료로부터 도출된다. 과도상태에 있어서는 노내및 노외중성자 측정기의 반응사이에 존재하는 선형적 관계로부터 물리적인 상관식을 개발하였다. 이 모델을 사용할 경우 제어봉의 위치가 크게 변하는 축방향 출력과도현상을 예측하는 1차원적 중성자 확산이론 프로그램의 신뢰도가 크게 향상된다.

Nomenclature

ϕ	1-energy group neutron flux(#/cm^2. sec)
ϕ^1	fast neutron flux(#/cm^2. sec)
ϕ^2	thermal neutron flux(#/cm^2. sec)
K^∞	infinite multiplication factor
K_{eff}	effective multiplication factor
M^2	migration area(cm^2)
B^2	radial leakage(cm^{-2}) as used in the RMS (see Section II. 2)
B_r^2	transverse buckling(cm^{-2})
D^1	fast diffusion coefficient(cm)
D^2	thermal diffusion coefficient(cm)
$\sum_a^1$	fast absorption cross section(cm^{-1})
$\sum_a^2$	thermal absorption cross section(cm^{-1})
$\sum_r$	fast to thermal removal cross section(cm^{-1})
$\nu\sum_f^1$	fast fission cross section(cm^{-1})
$\nu\sum_f^2$	thermal fission cross section(cm^{-1})

I. Introduction

The nuclear design of typical PWR has depended on the 1-dimensional(1-D) diffusion model to calculate practically the core average axial power distributions. This type of calculations demand significantly less computing time than the 2-dimensional (2-D) or 3-dimensional (3-D) core analysis. But the resulting data contain sufficient information about the core neutronic behaviors during normal operations and operational transients since the core radial power distributions are relatively monotonous and easily bounded by the design.

There is also an increasing need for this kind of program on the site to help operators to control their reactor in a predictive way especially during load follow operations. The 1-D model actually implemented on the site-computer executes the principal functions of the computer-aided power control system(CAP)[1] or the reactor management system(RMS)[2]. The minimal or maximal change of boron concentration, the required range of control rod displacement, the axial power imbalance or distribution, and the poison buildups after reactor trip can be calculated fast enough to accommodate the actual variations of core physical conditions.

The 1-D diffusion models[3][4] currently used by major vendors of PWR core are basically similiar to each other in that they are based on the 2-group diffusion equations incorporating pointwise feedback models. Although they have been successfuly employed either as a constituent tool of 1D-2D synthesis method[5] or as a simulation model of free-running xenon oscillations, their incapability of simulating relatively complicated load follow manoeuvres have been also noted: the axial power distributions calculated by one of the current models have been far away from those by a 3-D diffusion model.

The most important reason for this poor result is that a core average transverse buckling is applied to all axial nodes without consideration of local variations of neutronic conditions. The average or homogeneous buckling method fails where there exist large displacements of control rods. In his 1-D analysis of load follow operation with homogeneous buckling T. Morita[5] changed artificially his control rod positions from those used in 3-D reference calculations in order to adjust the axial power distributions to the reference ones. In certain cases[6] it has been necessray to introduce axial height-dependent bucklings specific to a given core condition so as to reduce the penalty to be imposed on the reactor power capability because of deficiencies in models. But it has been arbitrary and demanded experiences to determine such bucklings.

The transverse buckling is employed as a parameter of correcting the predictions of the CAP or the RMS. It is updated periodically to match the predicted power distributions to the measured ones. But no analytical model for transient core has been developed and the updating is done experientially.

In this paper an axial height-dependent transverse buckling model generally applicable to all reactor conditions is presented and tested. For normal depletion calculations the bucklings are obtained from an available 3-D depletion file which is generated for some other purposes. For transient core a correlation is developed from physical reasonings based on the observed relationship between in-core and ex-core detectors. A procedure of executing systematically a series of calculations from the steady-state to the transient state is also proposed. Extensive verifications for various reactor conditions are performed against the results of lengthy 3-D calculations.

II. Analytical Model

II. 1. Summary of the 1-Dimensional Diffusion Theory Program, DDID

This model has been developed from a 3-D diffusion program so as to study the operational transients with conveniences. It is in fact the updated version of the program that has been used to simulate the free-running xenon oscillations in Ref. 8. The governing equations are derived from their 3-D versions as shown in Appendix, where we find clearly the axial height-dependency of transverse bucklings. An explicit treatment of control rod movement and a simplified simulation of boration and dilution are added. The search on one of such important parameters as control rod position, soluble boron concentration and inlet temperature to get a required reactivity change is then easily perfo-rmed.

A burnup-dependent macroscopic cross section table is provided as inputs for each burnup cycle. This table is generated through the procedure shown in Fig. 1. The resulting cross sections are representative of radially homogenized axial core so that the comparison between the 1-D model and the 3-D model could be made without any bias.

II. 2. Transverse Buckling for Steady-States

In the RMS the 1-D model is based on the following 1-group diffusion equation:

$$\frac{d^2\phi(z)}{dz^2}+\left[\frac{K^{\infty}(z)-1}{M^2(z)}-B^2(z)\right]\phi(z)=0 \tag{II. 2-1}$$

At the initial state the calculated power distribution is made to coincide with the measured one by defining the radial leakage as follows:

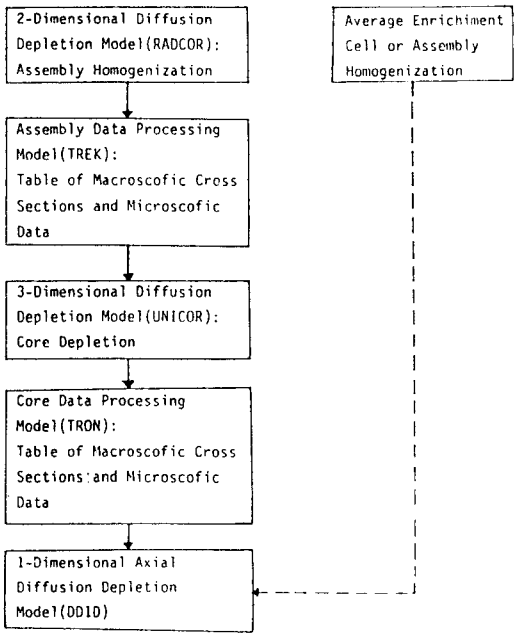

Fig. 1. Illustration of Nuclear Data Generation Procedure for 1-Dimensional Axial Diffusion Depletion Model

$$B^2{}_0(z)=\frac{1}{\phi_0(z)}\frac{d^2\phi_0(z)}{dz^2}+\frac{K_0^{\infty}(z)-1}{M_0{}^2(z)} \tag{II. 2-2}$$

where ϕ_0 is determined from the measurement.

If the measured flux distribution is not available the radial leakage at the initial state can be evaluated from a calculated 3-D flux distribution. This is the procedure adopted in this paper.

From the available 3-D depletion file for a given burnup cycle the transverse buckling corresponding to an axial node is calculated with the following analytical model. Assuming the spatial separability of leakage terms, we can write the 2-group diffusion equations for an axial node k as follows:

$$\int_{S_k}J_z{}^1\cdot ds+\int_{Z_k}J_r{}^1\cdot ds+\int_{V_k}(\Sigma_a{}^1+\Sigma_r)\phi^1 dv=\frac{1}{K_{eff}}\int_{V_k}(\nu\Sigma_f^1\phi^1+\nu\Sigma_f^2\phi^2)dv \tag{II. 2-3}$$

$$\int_{S_k}J_z{}^2\cdot ds+\int_{Z_k}J_r{}^1\cdot ds+\int_{V_k}\Sigma_a^2\phi^2 dv=\int_{V_k}\Sigma_r\phi^1 dv \tag{II. 2-4}$$

where $J_z^i = -D^i \partial\phi/\partial z$

$J_r^i = -D^i \partial\phi^i/\partial r$

S_k=area of radial plane at axial node k

Z_k=axial mesh width of axial node k

V_k=volume of axial node k

Using the bare reactor theory the second term on the left hand-side is approximated:

$$\int_{Z_k} J_r^i \cdot ds = -\int_{V_k} \frac{\partial}{\partial r} D^i \frac{\partial}{\partial r} \phi^i dv = (B_r^2)_k^i \int_{V_k} D^i \phi^i dv \qquad \text{(II. 2-5)}$$

Then the buckling for group 1 at axial elevation z is,

$$(B_r^2)_k^1 = \frac{\frac{1}{K_{eff}} \int_{V_k} (\nu\Sigma_f^1\phi^1 + \nu\Sigma_f^2\phi^2) dv - \int_{V_k} (\Sigma_a^1 + \Sigma_r)\phi^1 dv - \int_{S_k} J_z^1 \cdot ds}{\int_{V_k} D^1\phi^1 dv} \qquad \text{(II. 2-6)}$$

The buckling for group 2 is obtained in the same way:

$$(B_r^2)_k^2 = \frac{\int_{S_k} J_z^2 \cdot ds - \int_{V_k} \Sigma_a^2\phi^2 dv + \int_{V_k} \Sigma_r\phi^1 dv}{\int_{V_k} D^2\phi^2 dv} \qquad \text{(II. 2-7)}$$

The following equivalence relation is used to form a 1-group buckling:

$$(B_r^2)_k^1 \int_{V_k} D^1\phi^1 dv + (B_r^2)_k^2 \int_{V_k} D^2\phi^2 dv = (B_r^2)_k \int_{V_k} (D^1\phi^1 + D^2\phi^2) dv \qquad \text{(II. 2-8)}$$

Then,

$$(B_r^2)_k = \frac{\frac{1}{K_{eff}} \int_{V_k} (\nu\Sigma_f^1\phi^1 + \nu\Sigma_f^2\phi^2) dv - \int_{V_k} (\Sigma_a^1\phi^1 + \Sigma_a^2\phi^2) dv - \int_{S_k} (J_z^1 + J_z^2) \cdot ds}{\int_{V_k} (D^1\phi^1 + D^2\phi^2) dv} \qquad \text{(II. 2-9)}$$

The transverse buckling defined by Eq. (II. 2-9) has the effect of compensating for the missing radial dimension in the 1-D model to some extents. But it is unavoidable to have small discrepancies in axial power distributions between the 1-D model and the 3-D model. A simple way to get rid of this problem is to apply a linear weighting function to the axial distribution of the above-calculated bucklings as follows:

$$(B_r^2(z_k))_0 = W(z_k) \cdot (B_r^2)_k \qquad \text{(II. 2-10)}$$

$$W(z) = a \cdot (z - 0.5H) + 1.0 \qquad \text{(II. 2-11)}$$

where $(B_r^2(z_k))_0$=weighted transverse buckling

a=slope of linear weighting function $W(z)$

H=active core height

The weighting function is determined at the end of a few 1-D calculations with the slope a updated each time until the 1-D prediction coincides with the 3-D one. This function can also be used to adjust the initial states of the 1-D model to the measured state if the implementation is made on the site-computer.

II. 3. Physical Correlation for Transient States

In power transients like load follow operations the positions of control rods and the axial distributions of power, moderator density, and xenon are frequently varied. These parameters affect the radial leakage of neutrons or the transverse buckling in such a non-linear way that an analytical model accounting for all the effects is difficult to derive.

Again taking the example of the RMS the radial leakage in transients is obtained from the initial-state leakage as follows:

$$B^2(z) = B_0^2(z) + C(U - U_0) \qquad \text{(II. 3-1)}$$

where

C=constant

U_0=void fraction at the initial state

U=predicted void fraction

As we can see, this equation takes into account only the state variation due to the void fraction change. The effects of the other important par-

ameters must be considered in the initial-state leakage. This means that we must have a large set of initial-state leakages relating to the various core conditions.

To circumbent this difficulty a different approach is made and described in the following paragraphs.

Since the leakage neutrons contribute directly to the ex-core neutron detector responses, it can be logically inferred that the axial distribution of response magnitudes is the same as that of leakage neutrons. Using the 2-group method in Section Ⅱ.2 this means:

$$B_r^2(z)D^1(z)\phi^1(z)+B_r^2(z)D^2(z)\phi^2(z)=R(z) \quad (\text{Ⅱ}.3\text{-}2)$$

where $R(z)$ is the detector response properly normalized at axial location z.

It has been found[9] that there exists a linear relationship between the axial power imbalance measured by ex-core detector and that by in-core detector or that really existing in the core (also see Fig. 2). This can be expressed as follows:

$$\int_{L/2}^{L}R(z)dz-\int_{0}^{L/2}R(z)dz=\int_{L/2}^{L}C(z)P(z)dz-\int_{0}^{L/2}C(z)P(z)dz \quad (\text{Ⅱ}.3\text{-}3)$$

where L=active core height

$C(z)$=proportionality function

$P(z)$=relative power at axial location z.

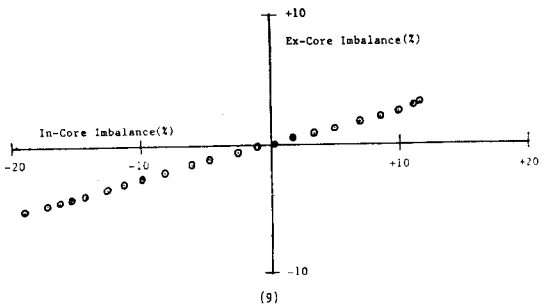

(9)

Fig. 2. Axial Power Imbalances Measured by Ex-Core Neutron Detectors vs. by In-Core Detectors

The Eq. (Ⅱ.3-3) relates the detector response imbalance to the power imbalance. This relation can be satisfied if,

$$R(z)=C(z)P(z) \quad (\text{Ⅱ}.3\text{-}4)$$

In real systems the ex-core detectors are calibrated periodically during core depletion according to the incore measurements. So we assume that $C(z)$ be function of core burnups.

From Eq. (Ⅱ.3-2) and Eq. (Ⅱ.3-4) we obtain the transverse buckling:

$$B_r^2(z)=\frac{C(z)P(z)}{D^1(z)\phi^1(z)+D^2(z)\phi^2(z)} \quad (\text{Ⅱ}.3\text{-}5)$$

The axial power and flux distributions are those really existing in the core. But we assume that they can be approximated by the calculated one so that the transverse buckling might be generated during transient calculations.

To take into account the effect of varying power level on the leakage of neutrons a parameter dominating neutron transport and also reflecting core thermal change is searched. Since the water density increasing due to thermal power decrease will augment the moderation of fast neutrons and reduce their leakage, the equation is simply modified as follows:

$$B_r^2(z)=\frac{C(z)P(z)}{D^1(z)\phi^1(z)+D^2(z)\phi^2(z)}\cdot\frac{1}{\rho(z)} \quad (\text{Ⅱ}.3\text{-}6)$$

where $\rho(z)$=axial distribution of water density

The proportionality function $C(z)$ is determineds from initial power distribution, for example, that resulting from all rods-out depletion calculation:

$$C(z)=\frac{(D_0^1(z)\phi_0^1(z)+D_0^2(z)\phi_0^2(z))\cdot(B_r^2(z))_0}{P_0(z)}\cdot\frac{}{\rho_0(z)} \quad (\text{Ⅱ}.3\text{-}7)$$

The proportionality function defined by Eq. (Ⅱ.3-7) contains the information about the characteristics of core states in terms of radial leakage at a given burnup. This is due to the fact that the term $(B_r^2(z))_0$ is evaluated from a 3-D power distribution. The effects of varying

control rod positions and axial distributions of other parameters are supposed to be all accounted for by the Eq.(Ⅱ.3-6), which is based on transient power and flux distributions.

III. Application and Results

The process of executing a series of calculations from the initial steady-state to the transient condition are procedeeded as follows:

1. For a given depletion cycle the initial bucklings are calculated from the available 3-D depletion file.

2. It is then corrected through the application of weighting function which is determined at the end of a few 1-D calculations.

3. The 1-D depletion calculation is done for each cycle and a set of burnup-dependent weighted bucklings are determined. Also the results of this calculation constitute the initial conditions in the 1-D model.

4. At a given burnup step various steady-states or transients are simulated departing from the initial conditions.

The advantageous feature of this procedure is that the once set-up initial condition in the 1-D model is a general one: it is specific only to the core burnups.

The 1-D model with the axial height-dependent buckling($B_r^2(z)$) is confronted with reactor conditions of varying burnups and power levels in normal all rods-out depletion and in load follow transients. For the same conditions the 3-D model and the 1-D model with homogeneous buckling($B_{r_0}^2$) are run to obtain reference values.

The transient modelled is 12-3-6-3 type load follow operation during cycle-1 of Kori Unit 1 reactor. The power levels are varied from 100% to 70% or 50% and the conditions beyond normal operational limits are also assumed to see the validity the model in extreme cases. Shown

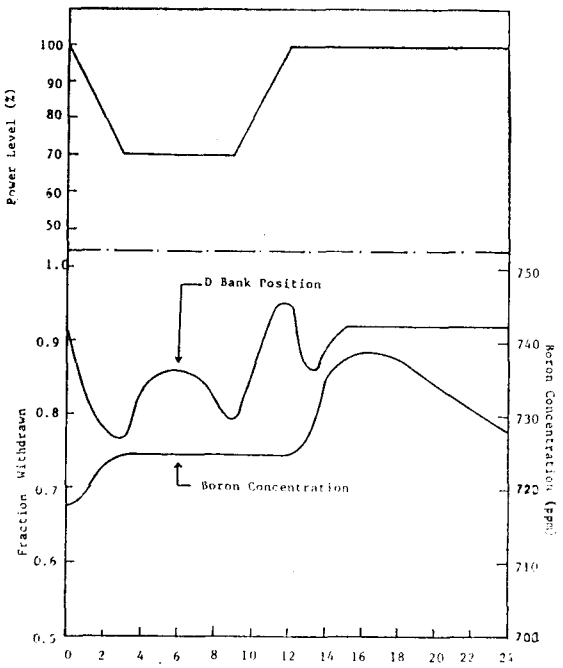

Fig. 3. Typical Variation of Control Bank D Position Requiring Minimum Action on Boron Concentration during 12-3-6-3 Type Load Follow Operation

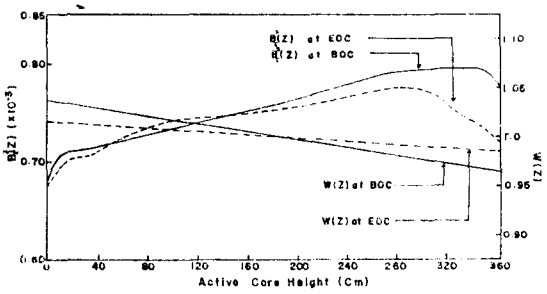

Fig. 4. Axial Height-Dependent Buckling at BOC and EOC of Cycle-1 Kori Unit-1

in Fig. 3 is a typical variation of control rod positions and boron concentrations during power level changes from 100% to 70% and 70% to 100%.

The following paragraphs summarize the calculational results:

1. In Fig. 4 and Fig. 5 the bucklings for BOC and EOC of cycle 1 and cycle 2 obtained from 3-D depletion file are shown along with the weighting function $W(z)$. When these bucklings are used for the 1-D depletion, the res-

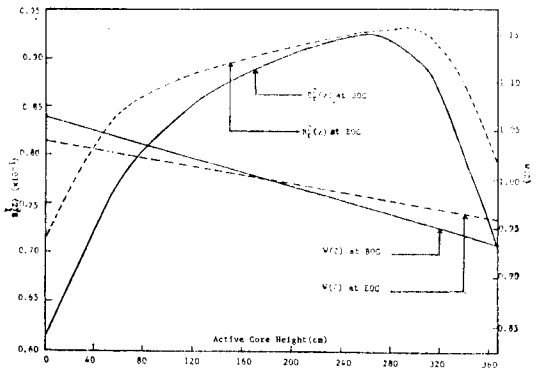

Fig. 5. Axial Height-Dependent Radial Buckling at BOC and EOC of Cycle-2/Kori Unit-1

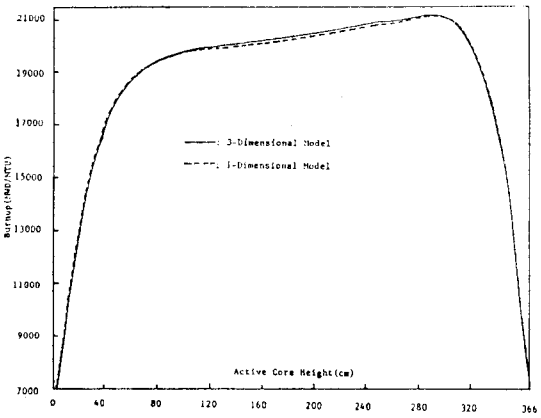

Fig. 6. Comparison of Burnup Distribution at EOC of Cycle-1/Kori Unit-1 between 1-Dimensional Model and 3-Dimensional Model

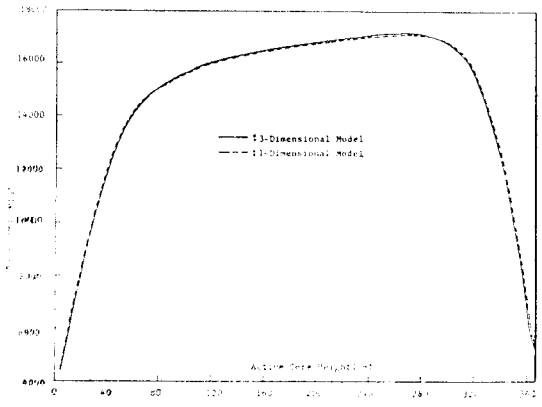

Fig. 7. Comparison of Burnup Distribution at EOC of Cycle-2/Kori Unit-1 between 1-Dimensional Model and 3-Dimensional Model

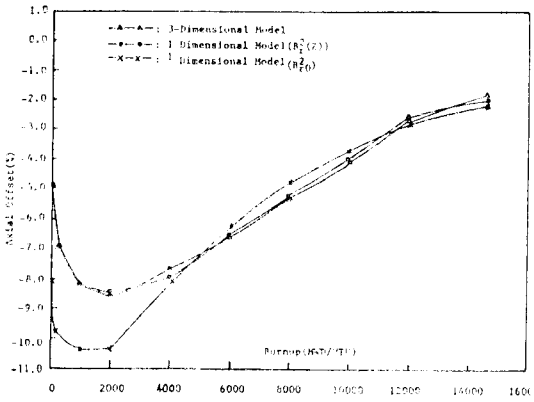

Fig. 8. Evolution of Axial Offset in HFP, ARO, EQ. Xenon Condition during Cycle-1/Kori Unit-1, Calculated by 1-Dimensional Model vs. 3-Dimensional Model

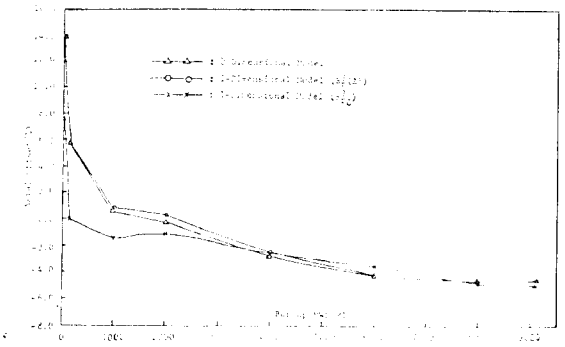

Fig. 9. Evolution of Axial Offset in HFP, ARO, EQ. Xenon Condition during Cycle-2/Kori Unit 1, Calculated by 1-Dimensional Model vs. 3-Dimensional Model

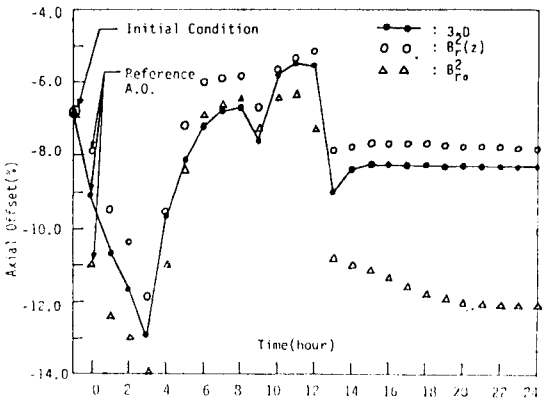

Fig. 10. Comparison of Axial Offsets during 100-70-100 Load Follow Operation Simulated at BOC of Cycle-1/Kori-1

ulting burnup distributions at EOC of each cycle are presented in Fig. 6 and Fig. 7 in comparison with references. The evolution of axial power imbalance or offset(A.O.) for each cycle is also presented in Fig. 8 and Fig. 9.

It can be pointed out clearly that the depletion with $B_r^2(z)$ is necessary to obtain correct burnup and poison distributions since they are affected directly by the power distributions.

2. In Fig. 10 and Fig. 11 the evolutions of A.O. during load follow operations respecting the operational limits are shown for BOC and MOC of cycle 1 when the power level is varied from 100% to 70% and from 70% to 100%. Another transient with power level change from 100% to 50% and from 50% to 100% is presented in Fig. 12.

For all the cases tested the results with $B_r^2(z)$ are much better than those with $B_{r_0}^2$. This fact is more eminent in the high power range. Because the limiting power distributions are normally produced in the resumed high power region (namely 100% nominal power) the good agreement acquired with $B_r^2(z)$ is significative. Shown in Fig. 13 is the evolution of axial peaking factors during 3 days of load follow operations at MOC of cycle 1 with power level change from 100% to 70% and from 70% to 100%. The maximum percent error with $B_r^2(z)$ model is of 2.8% at 48 hours while at this time that with $B_{r_0}^2$ model is of 9.0%.

3. In Fig. 14 the evolution of axial offsets during load follow operation violating the normal operational limits is shown for EOC of cycle 1. The power level is varied from 100% to 70% and from 70% to 100%. Again the results with $B_r^2(z)$ model is far better than that with $B_{r_0}^2$ model. With regard to the axial peaking factors shown in Fig. 15 it is remarked that the percent

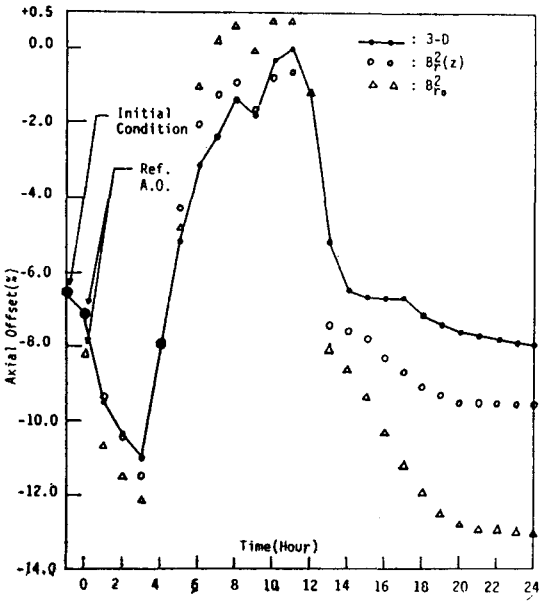

Fig. 11. Comparison of Axial Offsets during 100-70-100 Load Follow Operation Simulated at MOC of Cycle-1/Kori-1

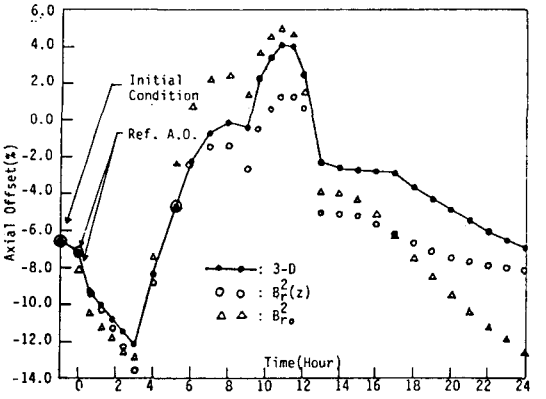

Fig. 12. Comparison of Axial Offsets during 100-50-100 Load Follow Operation Simulated at MOC of Cycle-1/Kori-1

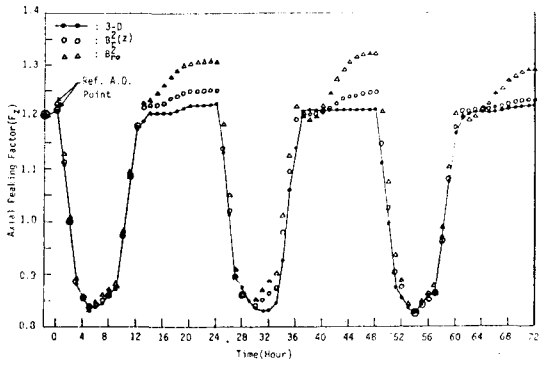

Fig. 13. Comparison of Axial Peaking Factors during 100-70-100 Load Follow Operation Simulated at MOC of Cycle-1/Kori-1

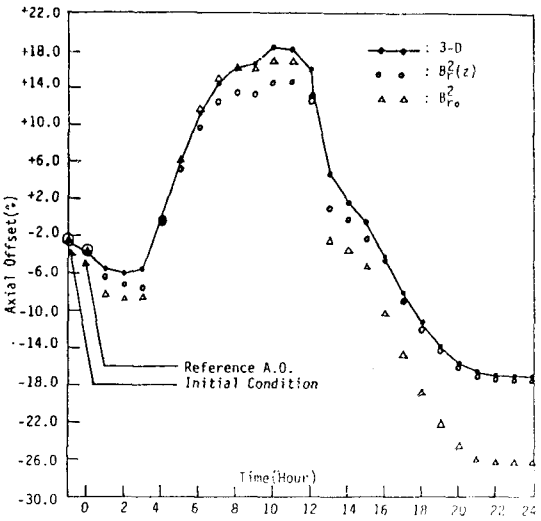

Fig. 14. Comparison of Axial Offsets during 100-70-100 Load Follow Operation Simulated at EOC of Cycle-1/Kori-1

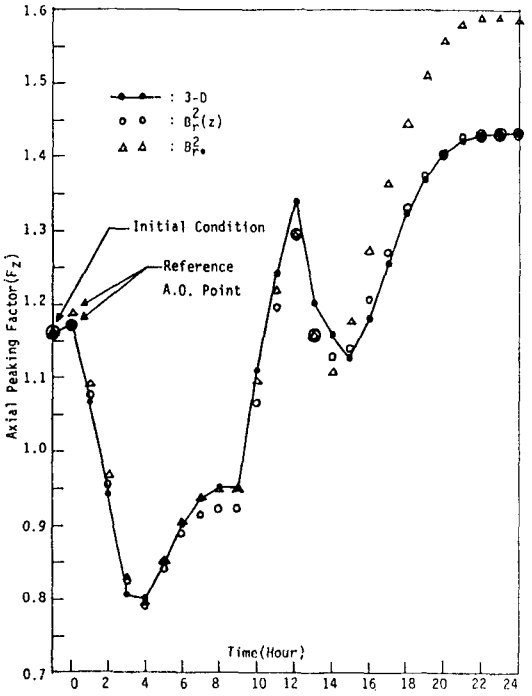

Fig. 15. Comparison of Axial Peaking Factors during 100-70-100 Load Follow Operation Simulated at EOC of Cycle-1/Kori-1

error at the end of the 1st day in load follow operation is of 0.07% for $B_r^2(z)$ model and of 11% for $B_{r_0}^2$ model.

4. It is generally observed that the results of the 1-D model are more penalizing than those of the 3-D model at the high power level: the axial peaking factor with $B_r^2(z)$ is slightly larger than the 3-D reference one and that with $B_{r_0}^2$ is much larger.

IV. Conclusion

The axial height-dependent buckling model is developed for the analysis of normal core depletion and power transients including load follow operations in the 1-D diffusion depletion program. The procedure of utilizing this model for a series of calculations from the initial steady-states to the transients is set up. From the test results at various core burnups and power levels the following conclusions are drawn:

1. The reliability of the 1-D diffusion theory program in predicting axial power transients accompanying important variations of control rod positions can be improved by using the present model.

2. The results with the present model are much more accurate than with the conventional homogeneous buckling model.

3. If this model is applied to the core design the penalty on the reactor power capability due to the deficiency in the calculaional method will be surely reduced.

The 1-dimensional diffusion program with this model and the procedure developed can be implemented on the site-computer to enhance the load follow capability of PWR.

Appendix

The 1-*D* axial diffusion model is employed to analyse the radially homogenized axial core. Consistently done with this fact is the derivation of the 1-*D* diffusion equations as used in the 1-*D* code.

The 2-group diffusion equation for an axial node k in the 3-*D* version has the form:

$$\int J^1 \cdot dS + \int_{V_k} (\Sigma_a^1 + \Sigma_r)\phi^1 dv = \frac{1}{K_{eff}} \int_{V_k} (\nu\Sigma_f^1\phi_1 + \nu\Sigma_f^2\phi^2)\, dv \tag{A-1}$$

$$\int J^2 \cdot dS + \int_{V_k} \Sigma_a^2 \phi^2 dv = \int_{V_k} \Sigma_r \phi^1 dv \tag{A-2}$$

The lst term on the left hand side of both equations are approximated as follows:

$$\int J^i \cdot dS = \int J_r^i \cdot dS + \int J_z^i \cdot dS = \int_{V_k} \frac{\partial}{\partial r} J_r^i dv + \int J_z^i \cdot dS$$

$$= -\int_{V_k} \frac{\partial}{\partial r} D^i \frac{\partial}{\partial r} \phi^i dv + \int J_z^i \cdot dS = (B_r^2)_k^i \int_{V_k} D^i \phi^i dv + \int J_z^i \cdot dS \tag{A-3}$$

The other terms are radially homogenized:

$$\int_{V_k} \Sigma_x^i \phi^i dv = \int_{Z_k} \int_{S_k} \Sigma_x^i \phi^i ds dz = S_k \int_{Z_k} \overline{\Sigma^i{}_x \phi^i} dz \tag{A-4}$$

where $\overline{\Sigma^i{}_x \phi^i} = \int_{S_k} \Sigma_x^i \phi^i dS / \int_{S_k} dS$

As well we homogenize the second term on the right hand side of Eq. (A-3):

$$\int J_z^i \cdot dS = \int \nabla \cdot J_z^i dv = \int_{Z_k} \int_{S_k} \nabla \cdot J_z^i dS dz = \int_{Z_k} \nabla \cdot \int_{S_k} J_z^i dS dz$$

$$= \int_{Z_k} \nabla \cdot \bar{J}_z^i S_k dz = S_k \int_{S_z} \bar{J}_z^i \cdot dS_z \tag{A-5}$$

where $\bar{J}_z^i = \int_{S_k} J_z^i \cdot dS / \int_{S_k} dS$

S_Z = unit area

Eq. (A-3), (A-4), and (A-5) are inserted into Eq. (A-1), and (A-2) and the resulting equations are rearranged:

$$\int_{S_z} \bar{J}_z^1 \cdot dS_Z + \int_{Z_k} (\overline{\Sigma^1{}_a \phi^1} + \overline{\Sigma_r \phi^1}) dz + (B_r^2)_k^1 \int_{Z_k} \overline{D^1 \phi^1} dz = \frac{1}{K_{eff}} \int_{Z_k} (\overline{\nu\Sigma^1{}_f \phi^1} + \overline{\nu\Sigma^2{}_f \phi^2})\, dz \tag{A-6}$$

$$\int_{S_z} \bar{J}_z^2 \cdot dS_z + \int_{Z_k} \overline{\Sigma^2{}_a \phi^2} dz + (B_r^2)_k^2 \int_{Z_k} \overline{D^2 \phi^2} dz = \int_{Z_k} \overline{\Sigma_r \phi^1} dz \tag{A-7}$$

Assuming $\overline{\Sigma^i{}_x \phi^i} \cong \bar{\Sigma}_x{}^i \bar{\phi}^i$, we obtain the following 1-D equations:

$$\int_{S_z} \bar{J}_z^1 \cdot dS_z + \int_{Z_k} (\bar{\Sigma}_a^1 + \bar{\Sigma}_r) \bar{\phi}^1 dz + (B_r^2)_k^1 \int_{Z_k} \bar{D}^1 \bar{\phi}^1 dz = \frac{1}{K_{eff}} \int_{Z_k} (\nu\bar{\Sigma}_f^1 \bar{\phi}^1 + \nu\bar{\Sigma}_f^2 \bar{\phi}^2) dz \tag{A-8}$$

$$\int_{S_z} \bar{J}_z^2 \cdot dS_z + \int_{Z_k} \bar{\Sigma}^2{}_a \bar{\phi}^2 dz + (B_r^2)_k^2 \int_{Z_k} \bar{D}^2 \bar{\phi}^2 dz = \int_{Z_k} \bar{\Sigma}_r \bar{\phi}^1 dz \tag{A-9}$$

Eq. (A-8) and (A-9) show that the transverse buckling in the 1-D model has the axial height-dependency.

References

1. A. Darraud et al., "Pressurized Water Reactors: Towards Improved Maneuverability," Public Relations Department, FRAMATOME (Oct. 1984).
2. Tsutomu Otsuka et al., "The Development of the Reactor Management System," Nucl. Technology V. 59, P. 199 (Nov. 1982).
3. S. Altomare and G. Minton, "The PANDA Code," WCAP-7757-A, Westinghouse Electric Corporation (Sept. 1971).
4. A. Darraud, "ESPADON-A One-Dimensional 2 Groups Diffusion Depletion Code," TP/CN/77. 342, FRAMATOME(Oct. 1977).
5. T. Morita et al., "Topical Report-Power Distribution Control and Load Follow Procedures," WCAP-8403, Westinghouse Electric Corporation (Sept. 1974).
6. A.L. Casadei, "PWR Nuclear Design and Safety Analysis," IAEA Specialist Seminar, Daeduk/Korea(Sept. 1984).

7. H.J. Moon, "DD1D-A One-Dimensional 2 Group Steady-State Neutron Diffusion Theory Program," KAERI/TR-31/81, Korea Advenced Energy Research Institute(Dec. 1981).
8. H.J. Moon and K.I. Han, "PWR Core Stability against Xenon-Induced Spatial Power Oscillation," Journal of Korean Nucl. Soc., V. 14, No. 2(Jun. 1982).
9. E.R. Kane et al., "In-core and Out-Core Flux Relationships," Trans. Amer. Nucl. Soc. V. 17, P. 502 (1973).